Int J CARS
DOI 10.1007/s11548-014-1010-3

ORIGINAL ARTICLE

Semi-automatic MRI segmentation and volume quantification of intra-plaque hemorrhage

Hui Tang · Mariana Selwaness · Reinhard Hameeteman · Anouk van Dijk · Aad van der Lugt · Jacqueline C. Witteman · Wiro J. Niessen · Lucas J. van Vliet · Theo van Walsum

Received: 30 October 2013 / Accepted: 11 April 2014

Abstract
Purpose Intra-plaque hemorrhage (IPH) is associated with plaque instability. Therefore, the presence and volume of IPH in carotid arteries may be relevant in predicting the progression of atherosclerotic disease and the occurrence of clinical events. The aim of our work was to develop and evaluate a method for semi-automatic IPH segmentation in T1-weighted (T1w)-magnetic resonance imaging (MRI).
Material and methods IPH segmentation is performed by a regional level set method that models the intensity of the IPH and the background in T1w-MRI to be smoothly varying. The method only requires minimal user interaction, i.e., one or more mouse clicks inside the hemorrhage serve as initialization. The parameters of the method are optimized using a leave-one-out strategy by maximizing the Dice similarity coefficient (DSC) between manual and semi-automatic segmentations. We evaluated the IPH segmentation method on 22 carotid arteries; 10 of which were annotated by two observers and 12 were scanned twice within a 2 week period.
Results We obtained a DSC of 0.52 between the manual and level set segmentations on all 22 carotids. The inter-observer DSC on 10 arteries is 0.57, which is comparable to the DSC between the method and the manual segmentation (0.55). The correlation between the IPH volumes extracted from the level set segmentation and the manual segmentation is 0.88, which is close to the inter-observer volume correlation of 0.92. The reproducibility after rescanning 12 carotids yield an IPH volume correlation of 0.97. The robustness with respect to the initialization by manually clicking two sets of seed points in these 12 carotid artery pairs yields a volume correlation of 0.99.
Conclusion Semi-automatic segmentation and quantification of IPHs are feasible with an accuracy in the range of the inter-observer variability. The method has excellent reproducibility with respect to rescanning and manual initialization.

Keywords Carotid arteries · Atherosclerosis · Intra-plaque hemorrhage · Piecewise-smooth regional level set

H. Tang (✉) · R. Hameeteman · W. J. Niessen · T. van Walsum
Biomedical Imaging Group Rotterdam, Department of Medical Informatics, Erasmus MC, P.O. Box 2040,
3000 CA Rotterdam, The Netherlands
e-mail: tanghui.seu@gmail.com

H. Tang · M. Selwaness · R. Hameeteman · A. van Dijk · A. van der Lugt · W. J. Niessen · T. van Walsum
Department of Radiology, Erasmus MC, P.O. Box 2040,
3000 CA Rotterdam, The Netherlands

H. Tang · W. J. Niessen · L. J. van Vliet
Quantitative Imaging Group, Department of Imaging Physics, and Technology, Faculty of Applied Sciences, Delft University of Technology, Delft, The Netherlands

M. Selwaness · A. van Dijk · J. C. Witteman
Department of Epidemiology, Erasmus MC, P.O. Box 2040,
3000 CA Rotterdam, The Netherlands

Introduction

Atherosclerosis is one of the main underlying causes of cardiovascular events such as ischemic stroke, and a major cause of mortality and morbidity [8]. Atherosclerosis progresses with age and often remains asymptomatic prior to clinical events [8]. Many studies investigated the relation between plaque growth and various other factors, such as vessel geometry and plaque composition [6,15,17]. Recently, intra-plaque hemorrhage (IPH) was found to be associated with the increase in size of the necrotic core and lesion instability in coronary plaques [11] and therefore, IPH is considered as a high risk component of the vulnerable plaques

Published online: 12 May 2014

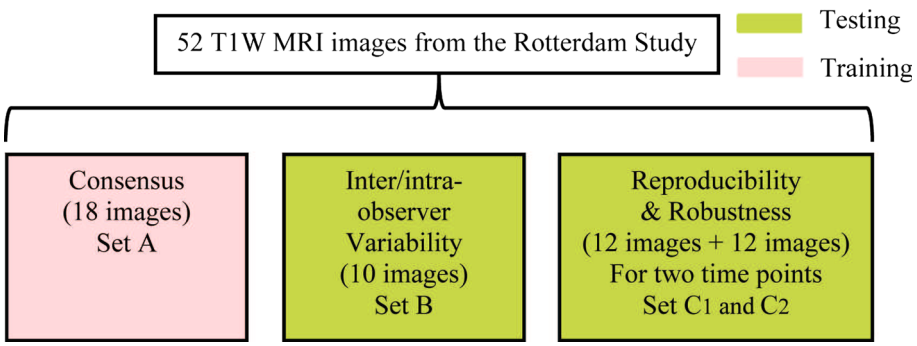

Fig. 1 Description of image data

[14]. IPH was also reported to be related to (recurrent) neurological events during follow-up [1]. Takaya et al. [16] found that the presence of IPH in carotid atherosclerotic plaques accelerated plaque progression over an 18-month period. The association between the size of IPH and plaque progression has not been investigated previously. MRI can be used for visualizing IPH [20]. It has been shown that high resolution MR has excellent capabilities for differentiating IPH from other carotid plaque tissues [3,4]. To study the association between IPH size and plaque progression, an MRI study was designed as part of a population-based study [9]. Purpose of our work was to develop a method for the precise and robust quantification of IPH volume from MRI data and evaluate it on those data.

Manual quantification of IPH (or other plaque characteristics) is a tedious procedure, prone to inter- and intra-observer variability. Therefore, there is a large interest in automated procedures for plaque assessment. Pattern recognition and machine learning methods play an important role in (semi-) automatic segmentation of plaque components [10,13,19]. Hofman et al. [10] quantified the relative area of all detected atherosclerotic plaque components, including IPH, using supervised classification techniques. Their method needs manual annotation of the inner and outer vessel wall to obtain a mask of the plaque and thus requires a significant amount of user interaction. Liu et al. [13] segmented plaque components based on morphology enhanced probability maps from in vivo magnetic resonance imaging (MRI), but IPH is not included in their work. Van Engelen et al. [19] segmented the plaque composition in ex vivo MRI using a machine learning method. Similar to the work by Hofman et al. [10] and Liu et al. [13], this method requires manual annotation of the inner and outer vessel wall.

In this paper, we present a semi-automatic approach to quantify the carotid IPH volume using manually selected seed points. The seed points are used to initialize a piecewise-smooth regional level set method that segments the IPH. Our main contributions are (1) we demonstrate the feasibility of precise IPH segmentation without vessel wall annotation and (2) we perform an extensive validation study to investigate the accuracy, and inter-scan reproducibility and robustness of the proposed semi-automatic IPH segmentation approach.

Materials and methods

Materials

Data description The data in this work are obtained from a prospective cohort study to investigate the prevalence, incidence, and risk factors of chronic diseases in an asymptomatic group of elderly aged 45 years and older [9]. In this study, 1,006 participants with a vessel wall thickness larger than 2.5 mm at plaque locations (determined by 2D ultrasound) underwent MR imaging of the carotid arteries [18]. The study procedures and consent forms were reviewed and approved by The Medical Ethics Committee of Erasmus MC, University Medical Center Rotterdam.

From this data set, we randomly selected 52 T1-weighted (T1w) MRI images (see Fig. 1) of 40 carotid arteries from 27 subjects among the participants who contain IPH. The 52 images were further divided into subsets, denoted by A, B, C_1, and C_2, based on the availability of manual reference data and re-scan data. Set A consists of 18 carotid arteries from 12 subjects with a consensus annotation by two observers. This set is used for parameter optimization. Ten data sets (set B) from six subjects have intra-/inter-observer annotations, and for 12 carotid arteries, we have images at two time points (C_1 and C_2), with <2 weeks between the acquisitions. The accuracy of the proposed method was evaluated using sets B and C_1 (22 data sets). The reproducibility and robustness of the method were evaluated on the 12 carotid arteries (24 image data sets) from 10 subjects for which two images are available (C_1 and C_2) and for which two observers provided seed points. An overview of the data used in this paper is shown in Fig. 1.

All scans were obtained with a 1.5-T scanner (GE Signa Excite II; GE Healthcare, Milwaukee, WI, USA) with a bilateral phased-array surface coil. The MRI acquisition parameters for the T1w MRI scans are as follows: a 3D gradient

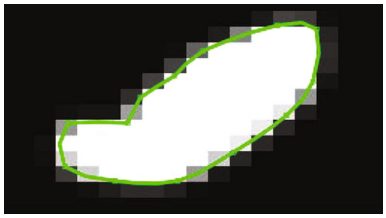

Fig. 2 An example of a manually drawn contour and the partial volume image generated from the manual contour

recalled echo sequence, scanned in the coronal plane, parallel to the common carotid artery, repetition time/echo time: 15.7/1.8 ms, field of view (FOV): $18 \times 18\,\mathrm{cm}^2$, matrix size: 192×180 in the coronal plane. The slice thickness is 1.0 mm, and the flip angle is 40°. The stenosis is measured manually using the NASCET (North American Symptomatic Carotid Endarterectomy Trial) criteria [2] and ranges from 0 to 90 % (23 % on average). All scans were reviewed by two independent physicians, both with 2 years experience in reading MRI, under supervision of a neuro-radiologist with more than 8 years of experience in MRI plaque analysis.

Reference standard The IPHs were manually annotated in axial slices using in-house developed software. Observers were able to zoom in and out and delineate the border by drawing contours around the IPHs per slice. For set A, two readers, R_1 and R_2, annotated the IPH border in consensus, yielding annotation $O^A_{\text{consencus}}$. For set B, reader R_1 performed the annotation two times, resulting in two annotations labeled as O^B_{11} and O^B_{12}, which enables the assessment of the intra-observer variability. The time interval between the two annotations is over 2 months. Reader R_2 performed the annotation once, resulting in one annotation labeled as O^B_2 to allow the assessments of the inter-observer variability. Reader R_1 also annotated sets C_1 and C_2 twice. The manual contours were used to create a partial volume image by calculating the fraction of the voxel inside the contour (a polygon) for every voxel in each slice. In the partial volume image, the intensity value ranges between 0 and 1, indicating the fraction of each voxel occupied by the IPH (Fig. 2). The manual method takes around 10 min per carotid artery.

Methods

The IPH segmentation is performed by a piecewise regional level set initialized by seed points. A region of interest is automatically generated around the seed points. The size of the region is defined by a box whose size is 15 voxels larger in all directions than the smallest bounding box that encloses all seed points. Figure 3 shows a slice through the 3D volume, the projected seed points, and the automatically cropped image.

For the semi-automatic IPH segmentation, we require a method that can deal with: (1) varying size of IPHs, (2) intensity variation within the IPH due to variations in plaque composition, and (3) intra-scan intensity variations. Based on these requirements, we chose a piecewise-smooth regional level set for this purpose [12]. The level set's energy function is

$$\begin{aligned} &E_{\mathrm{RSF}}(\phi(\boldsymbol{x})) \\ &= \lambda_1 \int \int K_\sigma(\boldsymbol{y}-\boldsymbol{x})(I(\boldsymbol{y}) - f_1(\boldsymbol{x}))H_1(\phi(\boldsymbol{x}))\mathrm{d}\boldsymbol{x}\mathrm{d}\boldsymbol{y} \\ &\quad +\lambda_2 \int \int K_\sigma(\boldsymbol{y}-\boldsymbol{x})(I(\boldsymbol{y}) - f_2(\boldsymbol{x}))H_2(\phi(\boldsymbol{x}))\mathrm{d}\boldsymbol{x}\mathrm{d}\boldsymbol{y} \\ &\quad +\upsilon|\nabla\phi(\boldsymbol{x})|, \end{aligned} \tag{1}$$

where $\phi(\boldsymbol{x})$ is a signed distance map which is negative inside the segmentation surface S, positive outside, and zero at the border. $H_1(\phi(\boldsymbol{x}))$ is the Heaviside function representing the current segmentation during the iteration process which has the value 0 inside the surface S and 1 outside, and $H_2(\phi(\boldsymbol{x}))$ is equal to $1 - H_1(\phi(\boldsymbol{x}))$. $K_\sigma(\boldsymbol{y}-\boldsymbol{x})$ is a Gaussian function that controls the size of a spherical region in which the intensity

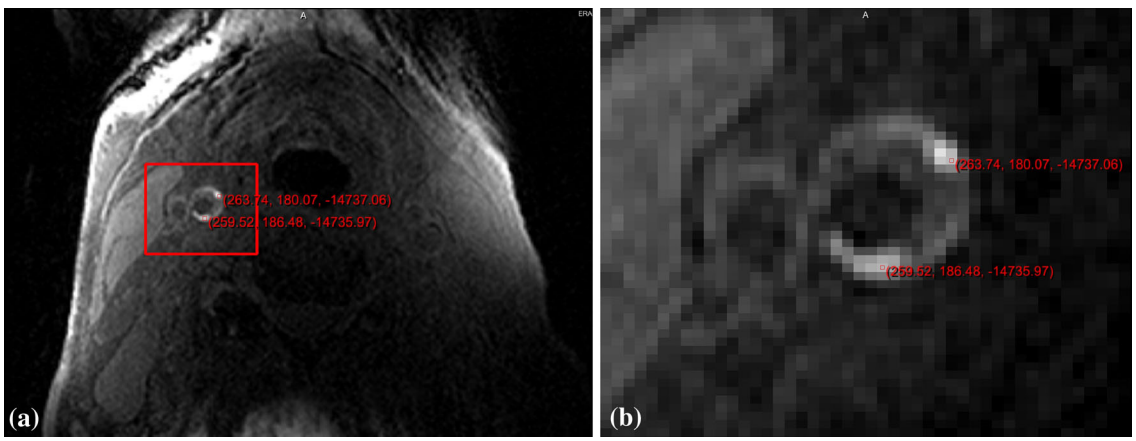

Fig. 3 **a** The original image overlaid by the automatic bounding box (*red*), **b** automatically cropped image using the clicked seed points

Table 1 The mean and standard deviation (SD) of the volumes in each dataset in testing

Dataset	B	C_1	C_2
O_{11} (mean/SD in μl)	79.8/86.7	59.7/62.7	117.2/111.6
O_{12} (mean/SD in μl)	75.0/95.5	–	–
O_2 (mean/SD in μl)	101.5/122.3	–	–
auto (mean/SD in μl)	133.0/141.9	132.4/122.8	149.9/160.1

inhomogeneity is ignored, a larger (smaller) scale σ assumes a homogenous intensity in a larger (smaller) local region and thus a less (more) severe intensity inhomogeneity. The term $f_i(\boldsymbol{x})$ $(i = 1, 2)$ denotes the estimated mean intensity as a function of image location. We use a local estimate $f_i(\boldsymbol{x})$ instead of a global constant to estimate the mean intensity in the fore- and background, in order to take intensity inhomogeneity into account. Li et al. used a standard gradient descent method to minimize Eq. 1, which upon convergence yields the final segmentation $\phi(\boldsymbol{x}) = 0$. In each iteration, we need to update $f_i(\boldsymbol{x})$, $i = 1, 2$ according to

$$f_i(\boldsymbol{x}) = \frac{K_\sigma(\boldsymbol{x}) * [H_i(\phi(\boldsymbol{x}))I(\boldsymbol{x})]}{K_\sigma(\boldsymbol{x}) * H_i(\phi(\boldsymbol{x}))}, \quad i = 1, 2$$

where $*$ denotes the convolution operation. A curvature term, weighted by v, is included to enforce the smoothness of the surface [5].

The method was implemented in itk (www.itk.org) and runs on a Linux workstation with 16 processors (AMD 6172, 12 cores, 2.1 GHz). The processing time is around 1 min per seed points. None of the processing steps uses a parallel implementation.

Experiments and results

Experiments are designed to determine both inter- and intra-observer variability and to determine the difference between the semi-automatic method and the observers. First, inter- and intra-observer variabilities are assessed. Subsequently, for the semi-automatic method, parameter settings for IPH segmentation are optimized on training set A. Then, the segmentation results are compared with the manual reference standard. This value is further compared with the inter-/intra-variability. Finally, the robustness and inter-scan reproducibility of the method are investigated. The mean and standard deviation of the volume in all the dataset for different annotations are listed in Tables 1, 2.

Inter- and intra-observer variability

The inter-observer Dice similarity coefficient (DSC) [7] is defined as the average of the two DSC's between the first observer's and the second observer's annotations and is found to be 0.57. The intra-observer DSC is defined as the DSC between the two annotations of the first observer and is equal to 0.62. Figure 4 shows the scatter plot of volume quantifications from these annotations. The intra-observer correlation of volume is 0.92, while the average correlation of the inter-observer correlation of volume is 0.95.

Table 2 The mean and standard deviation of the volume difference and mean absolute volume difference for the inter-/intra-observer variability, the accuracy assessment, the inter-scan reproducibility study, and the seed point robustness study

Analysis	Intra	Inter	Accuracy	Automatic reproducibility	Manual reproducibility	Seed point robustness
Difference (mean/SD in μl)	4.8/36.9	24.1/42.2	−61.3/70.7	−17.5/50.0	−57.5/94.1	−4.3/13.0
Absolute difference (mean/SD in μl)	23.8/27.6	26.1/40.9	63.3/68.9	30.7/42.5	81.0/72.8	8.1/11.0

Table 3 The results after parameter training, where the second row lists the average DSC on the training set, i.e., all subjects excluding the subject in the column

SubjectID	0	1	2	3	4	5	6	7	8	9	10	11
DSC (%)	51	48	48	41	49	49	47	49	48	48	52	48
λ_1	1	1	1	1	1	1	1	0.9	1	1	1	1
v	7e−3	7e−3	8e−3	7e−3	8e−3	8e−3	7e−3	10e−3	7e−3	8e−3	7e−3	7e−3
σ	0.1	0.1	0.1	0.1	0.1	0.1	0.1	0.1	0.1	0.1	0.1	0.1
DSC_L (%)	8	70	66	41	43	–	47	50	–	62	0	–
DSC_R (%)	48	49	–	–	56	38	76	35	–	58	48	55

The sixth and seventh rows show the DSC of the subject in the current column (test set) using these optimal parameter values. An entry listing the '–' sign indicates that the corresponding carotid artery does not have any IPHs. A DSC of '0' means that the semi-automatic segmentation method shrinks to a size of zero volume. DSC_L (DSC_R): DSC between the manual and the semi-automatic segmentation for the left (right) carotid artery

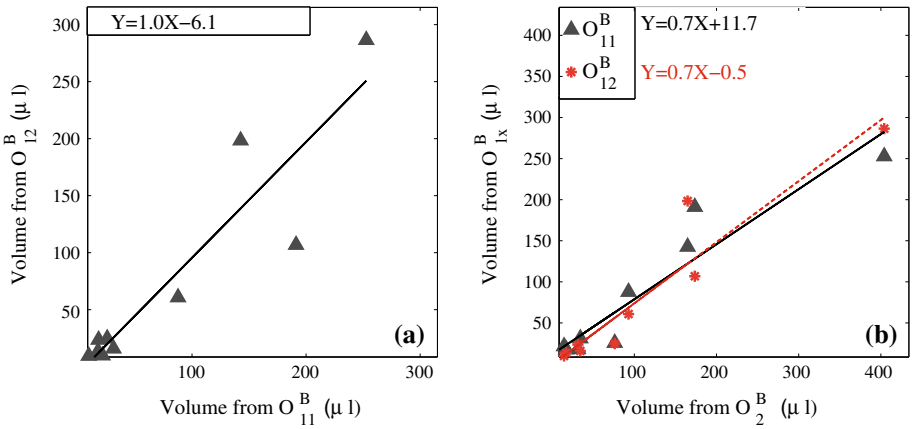

Fig. 4 Scatter plot of **a** the IPH volumes measured twice by the first observer and **b** the IPH volumes measured by the first observer and second observer

Parameter optimization

The semi-automatic segmentation method includes a number of parameters: the parameter λ_1 and λ_2 determines the weights of the internal and external intensity dissimilarity; v determines the weight of the curvature which controls the smoothness of the segmentation, and σ is the scale of the Gaussian function which controls the size of the region. The optimal value for these parameters was determined in a leave-one-out fashion on data set A. Since only the relative value of the internal and external weights, λ_1 and λ_2, and curvature weight v matters, we fixed λ_2 to be 1 and optimized the values for λ_1 and v, as well as the parameter σ. The curvature weight v was trained from 0.004 to 0.010 in 7 steps. The internal weight λ_1 was varied from 0.9 to 1.8 with a step size of 0.1. The Gaussian kernel scale σ was varied between 0.1 and 1 in two steps. We set the number of iterations to 200. The initial size of the segmentation is a sphere with a radius of 1 mm around the seed points. The leave-one-subject-out training results are shown in Table 3. The overall optimal values for IPH segmentation using the piecewise-smooth regional level set are $\lambda_1 = 1$, $v = 0.007$ and $\sigma = 0.1$ mm.

Accuracy

Three IPH segmentation results on the test sets (B and C_1) are shown in Fig. 5. We compared the automatically quantified volume to the average volume from three annotations in set B (10 images) and the only annotation in set C_1 (12 images); both are depicted by triangles in Fig. 6. We obtained a DSC of 0.53 with regard to the average manual volume in set B and the first observer in set C_1. The Pearson correlation coefficient between the manual and semi-automatic volumes is 0.88. Figure 6a also shows the scatter plot of the semi-automatic volume and the three annotations in set B. The difference between the annotations increases with volume.

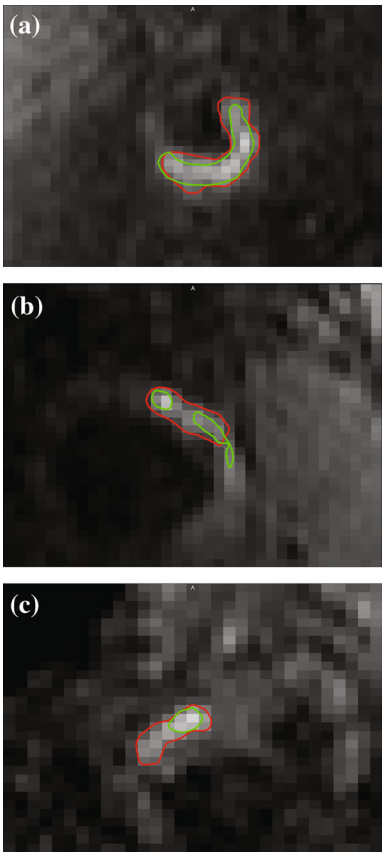

Fig. 5 IPH segmentation results; the manual segmentation in *green* and the semi-automatic segmentation in *red*, **a** Dice = 0.74, **b** Dice = 0.60, **c** Dice = 0.52

We compared our semi-automatic segmentation results for data sets B to the inter- and intra-observer variability. The average DSC between the semi-automatic method and the average of three annotations is 0.55, which is close to the inter-observer variability of 0.57. Figure 6 shows the scatter plot between the manual segmentation and the semi-automatic volumes, the Pearson correlation coefficient is 0.88.

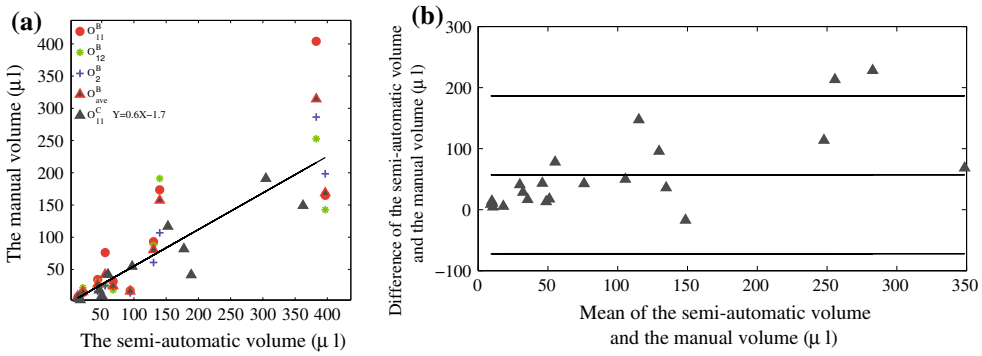

Fig. 6 **a** Scatter plot and the regression line between manual and semi-automatic volume and **b** Bland and Altman plot of the manual volume and semi-automatic volume in sets B and C_1

Inter-scan reproducibility and robustness

Reproducibility and robustness of the method with regard to rescanning and seed point selection were assessed by applying the method to the carotid arteries in sets C_1 and C_2. The Pearson correlation coefficient between the 12 pairs of volumes obtained by applying the semi-automatic (manual) segmentation to both timepoints with the semi-automatic segmentation for images acquired at two time points is 0.97, which is considerably higher than that between the manual annotation of two time points (0.71). The Bland and Altman plot in Fig. 7 shows that the **absolute** difference between the two volumes increases with the average size of the IPH. We performed a Wilcoxon's signed rank test between the 12 pairs of volumes obtained with the semi-automatic segmentation (manual segmentation) acquired at two different time points, the p value is 0.38 (0.04) at a confidence level of 95 %, indicating a good (poor) reproducibility of the imaging techniques and semi-automatic (manual) segmentation methods. The mean absolute difference between the volumes of the first and second scan obtained from the semi-automatic segmentation is 30.7 µl, whereas the mean absolute difference between the volumes of the first and the follow-up scans obtained from the manual segmentation is 81.0 µl, shown in Table 3. Figure 8 shows the scatter plot of the 12 pairs of manual volumes and the Bland and Altman plot.

We also studied the robustness of the method with respect to manual seed point selection on sets C_1 and C_2. Two observers independently selected two series of seed points with a time interval of more than 1 month. The Pearson correlation coefficient between volumes from two semi-automatic segmentations is 0.99, as seen in Fig. 9a. We also performed a paired t test between the 24 pairs of semi-automatic volumes acquired with two different initial seeds, the p value is 0.12 at a confidence level of 95 %, indicating a good robustness of this method with respect to the manual initialization. The average DSC between two semi-automatic segmentations is 0.88, and the mean absolute difference between the volumes obtained with two semi-automatic segmentations with two different sets of seed points is 8.1 µl, shown in Table 3.

Discussion and conclusion

We presented a semi-automatic IPH segmentation and quantification method that does neither require manual annotation of the inner or outer vessel wall nor preprocessing to correct for intensity inhomogeneities. The method segments IPHs

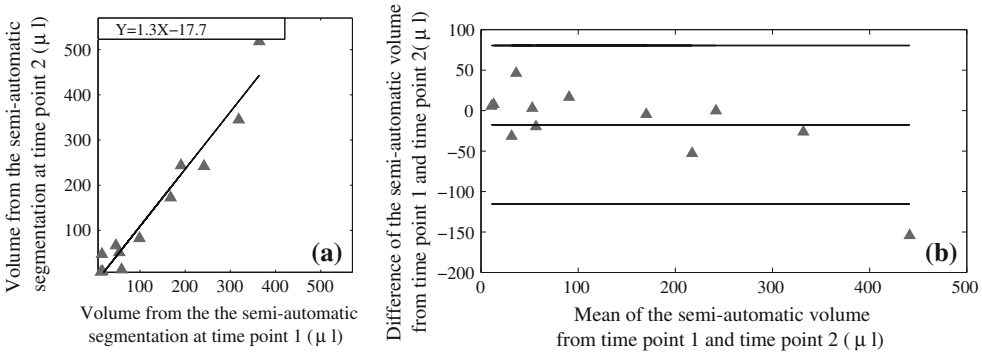

Fig. 7 **a** Scatter plot and **b** Bland and Altman plot of the semi-automatic volumes from two time points (sets C_1 and C_2)

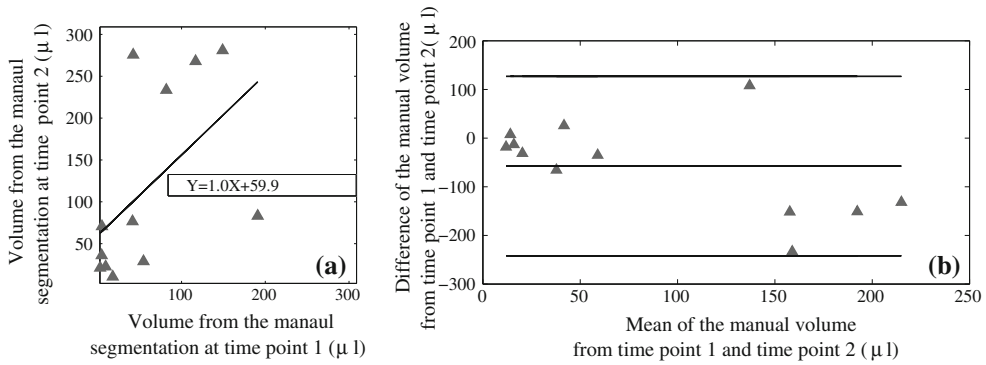

Fig. 8 **a** Scatter plot and **b** Bland and Altman plot of the manual volumes from two time points (sets C_1 and C_2)

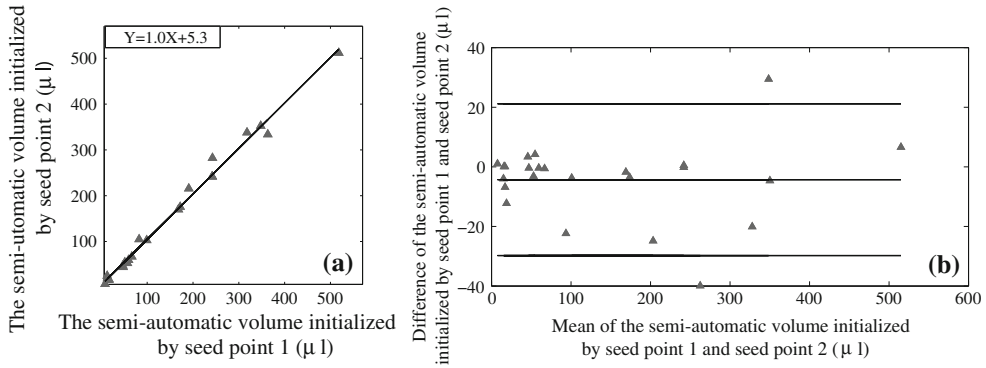

Fig. 9 **a** Scatter plot and **b** Bland and Altman plot of the semi-automatic volumes from two initializations (sets C_1 and C_2)

using a piecewise-smooth regional level set initialized by a set of manually clicked seed points. We trained the parameters of this segmentation using a leaving-one-out strategy on 18 images. The method is evaluated for accuracy on 34 images and for robustness and inter-scan reproducibility on 24 images.

We obtained a volume correlation of 0.88 between the semi-automatic segmentation and the manual segmentation in 10 data sets, which is slightly less than the inter-observer correlation. A robustness study with respect to the selection of seed points yielded a high volume correlation between the volumes obtained using two different seed points, which is better than the intra-observer correlation (*0.92*). The inter-scan reproducibility experiments showed that the segmented volumes of the semi-automatic method have a much higher reproducibility than those of the observers.

This study demonstrates that the manual annotation of IPH is subject to large observer variability. Therefore, the semi-automatic results can at best also have a moderate agreement with the manual reference standard. However, the robustness and inter-scan reproducibility of the semi-automatic method are better than the manual observations. This suggests that semi-automatic IPH volume quantification is to be preferred in clinical studies.

We found three existing alternatives [10,13,19] for IPH segmentation whose accuracy was evaluated by different metrics: area correlation [13], relative area difference and correlation [10], and classification statistics (AUC, PPV, NPV, sensitivity and specificity) [19]. Even though it is difficult to compare our method with the others due to the differences in evaluation metrics and data selection, we can state the following differences with previous studies: (1) the methods by [10,13,19] all need a manual segmentation of the inner and outer vessel wall to define a region of interest. In contrast, our method needs a few seed points as user inputs, which largely reduces the user interaction. (2) We performed a 3D segmentation, while Liu et al. [13] and Hofman et al. [10] performed a 2D segmentation. (3) All three methods [10,13,19] used a voxel-wise classification method to segment each plaque component, while we directly segment only the IPH using a levelset approach. The latter is expected to achieve subvoxel accuracy. Additionally, our study is the only one addresses reproducibility with respect to rescanning, which is essential for the application of the method in longitudinal studies.

This work has some limitations. We did not evaluate the robustness of the method with respect to scanner type. However, as there is a parameter training part involved, we expect that similar results can be obtained on different scanners, provided that a similar parameter training experiment with representative data from that scanner is performed.

We presented a semi-automatic IPH segmentation method, which gives IPH volume quantifications with an accuracy similar to manual annotation. In the robustness study as well as the reproducibility study, the quantifications obtained with the semi-automatic method are shown to be more robust and reproducible than those obtained from manual annotations. We thus demonstrated the feasibility of semi-automatic quantification of IPH volumes.

Conflict of interest Hui Tang, Mariana Selwaness, Reinhard Hameeteman, Anouk van Dijk, Aad van der Lugt, Jacqueline C Witteman, Wiro J Niessen, Lucas J van Vliet and Theo van Walsum declare that they have no conflict of interest.

Informed consent was obtained from all patients for being included in the study.

References

1. Altaf N, Daniels L, Morgan PS, Auer D, MacSweeney ST, Moody AR, Gladman JR (2008) Detection of intraplaque hemorrhage by magnetic resonance imaging in symptomatic patients with mild to moderate carotid stenosis predicts recurrent neurological events. J Vasc Surg 47(2):337–342. doi:10.1016/j.jvs.2007.09.064. http://www.sciencedirect.com/science/article/B6WMJ-4RPSH92-P/2/2bbdaed07bbb88aed06a6f8b190ddd08
2. Barnett HJ, Taylor DW, Eliasziw M, Fox AJ, Ferguson GG, Haynes RB, Rankin RN, Clagett GP, Hachinski VC, Sackett DL et al (1998) Benefit of carotid endarterectomy in patients with symptomatic moderate or severe stenosis. N Engl J Med 339(20):1415–1425
3. Bitar R, Moody AR, Leung G, Symons S, Crisp S, Butany J, Rowsell C, Kiss A, Nelson A, Maggisano R (2008) In vivo 3D high-spatial-resolution MR imaging of intraplaque hemorrhage. Radiology 249(1):259–267
4. Cappendijk VC, Cleutjens KBJM, Kessels AGH, Heeneman S, Schurink GWH, Welten RJTJ, Mess WH, Daemen MJAP, van Engelshoven JMA, Kooi ME (2005) Assessment of human atherosclerotic carotid plaque components with multisequence MR imaging: initial experience1. Radiology 234(2):487–492. doi:10.1148/radiol.2342032101. http://radiology.rsna.org/content/234/2/487.abstract
5. Caselles V, Kimmel R, Sapiro G, Sbert C (1997) Minimal surfaces based object segmentation. IEEE Trans Pattern Anal Mach Intell 19:394–398
6. Chambless LE, Heiss G, Folsom AR, Rosamond W, Szklo M, Sharrett AR, Clegg LX (1997) Association of coronary heart disease incidence with carotid arterial wall thickness and major risk factors: the atherosclerosis risk in communities (ARIC) study, 1987–1993. Am J Epidemiol 146(6):483–494
7. Dice LR (1945) Measures of the amount of ecologic association between species. Ecology 26(3):297–302
8. Epstein FH, Ross R (1999) Atherosclerosis: an inflammatory disease. N Engl J Med 340(2):115–126. http://dx.doi.org/10.1056/NEJM199901143400207
9. Hofman A, van Duijn CM, Franco OH, Ikram MA, Janssen HL, Klaver CC, Kuipers EJ, Nijsten TE, Stricker BHC, Tiemeier H et al (2011) The Rotterdam study: 2012 objectives and design update. Eur J Epidemiol 26(8):657–686
10. Hofman JMA, Branderhorst W, ten Eikelder H, Cappendijk V, Heeneman S, Kooi M, Hilbers P, ter Haar Romeny B (2006) Quantification of atherosclerotic plaque components using in vivo MR and supervised classifiers. Magn Reson Med 55(4):790–799. http://dx.doi.org/10.1002/mrm.20828
11. Kolodgie FD, Gold HK, Burke AP, Fowler DR, Kruth HS, Weber DK, Farb A, Guerrero L, Hayase M, Kutys R, Narula J, Finn AV, Virmani R (2003) Intraplaque hemorrhage and progression of coronary atheroma. N Engl J Med 349(24):2316–2325. http://www.nejm.org/doi/abs/10.1056/NEJMoa035655
12. Li C, Kao CY, Gore JC, Ding Z (2008) Minimization of region-scalable fitting energy for image segmentation. IEEE Trans Image Process 17(10):1940–1949
13. Liu F, Xu D, Ferguson MS, Chu B, Saam T, Takaya N, Hatsukami TS, Yuan C, Kerwin WS (2006) Automated in vivo segmentation of carotid plaque MRI with morphology-enhanced probability maps. Magn Reson Med 55:659–668
14. Selwaness M, van den Bouwhuijsen Q, Verwoert G et al (2013) Blood pressure parameters and carotid intraplaque hemorrhage as measured by magnetic resonance imaging: the Rotterdam study. Hypertension 61(1):76–81
15. Smedby Ö, Bergstrand L (1996) Tortuosity and atherosclerosis in the femoral artery: what is cause and what is effect? Ann Biomed Eng 24(4):474–480
16. Takaya N, Yuan C, Chu B, Saam T, Polissar NL, Jarvik GP, Isaac C, McDonough J, Natiello C, Small R, Ferguson MS, Hatsukami TS (2005) Presence of intraplaque hemorrhage stimulates progression of carotid atherosclerotic plaques: a high-resolution magnetic resonance imaging study. Circulation 111(21):2768–2775. http://circ.ahajournals.org/cgi/content/abstract/111/21/2768
17. Thomas JB, Antiga L, Che SL, Milner JS, Hangan Steinman DA, Spence JD, Rutt BK, Steinman DA (2005) Variation in the carotid bifurcation geometry of young versus older adults: implications for geometric risk of atherosclerosis. Stroke 36(11):2450–2456. http://stroke.ahajournals.org/cgi/content/abstract/36/11/2450
18. Van den Bouwhuijsen QJ, Vernooij MW, Hofman A, Krestin GP, van der Lugt A, Witteman JC (2012) Determinants of magnetic resonance imaging detected carotid plaque components: the Rotterdam study. Eur Heart J 33(2):221–229
19. Van Engelen A, De Bruijne M, Klein S, Verhagen H, Groen H, Wentzel J, Van der Lugt A, Niessen W (2011) Plaque characterization in ex vivo mri evaluated by dense 3D correspondence with histology. In: SPIE medical imaging, international society for optics and photonics, p 796329
20. Wasserman BA (2010) Advanced contrast-enhanced MRI for looking beyond the lumen to predict stroke: building a risk profile for carotid plaque. Stroke 41:S12–S16